https://doi.org/10.1595/205651322X16334238659301 *Johnson Matthey Technol. Rev.*, 2022, **66**, (3), 230–244

JOHNSON MATTHEY
TECHNOLOGY REVIEW

www.technology.matthey.com

# Review of Recent Progress in Green Ammonia Synthesis

## Decarbonisation of fertiliser and fuels *via* green synthesis

**Katie Smart**
Johnson Matthey, PO Box 1, Belasis Avenue, Billingham, TS23 1LB, UK

**Email:** katie.smart@matthey.com

**PEER REVIEWED**

Received 26th July 2021; Revised 29th September 2021; Accepted 1st October 2021; Online 5th October 2021

Most of the global production of ammonia requires fossil fuels and is associated with considerable greenhouse gas emissions. Replacing fossil fuel ammonia with green or zero-carbon ammonia is a major focus for academia, industry and governments. Ammonia is a key component in fertiliser but is also attracting increasing interest as a carbon-free fuel for the maritime sector and as a hydrogen vector. This review describes the use of green (electrolysed) hydrogen in conventional Haber-Bosch plants and predicts adoption of the technology by 2030. Further into the future, direct green ammonia synthesis by electrocatalytic and photocatalytic means may present a cost-effective alternative to the Haber-Bosch process. Electrocatalytic and photocatalytic routes to ammonia are reviewed, the catalytic systems are compared and their potential for meeting the likely demand and cost for ammonia considered.

## 1. Introduction

Ammonia is a vital commodity chemical incorporated into the fertilisers that are needed to feed the growing global population. The conventional industrial process to produce ammonia involves the conversion of hydrocarbons into hydrogen through purification, steam reforming, water-gas shift and separation. Nitrogen is incorporated from the air during secondary steam reforming. Ammonia is made in the Haber-Bosch process; a synthesis loop that operates at high pressure (150–350 bar) to favour the gaseous reaction of nitrogen and hydrogen and high temperature (400–450ºC) to promote the reaction kinetics (1). The reaction is catalysed by metallic iron. The process is summarised in **Figure 1**.

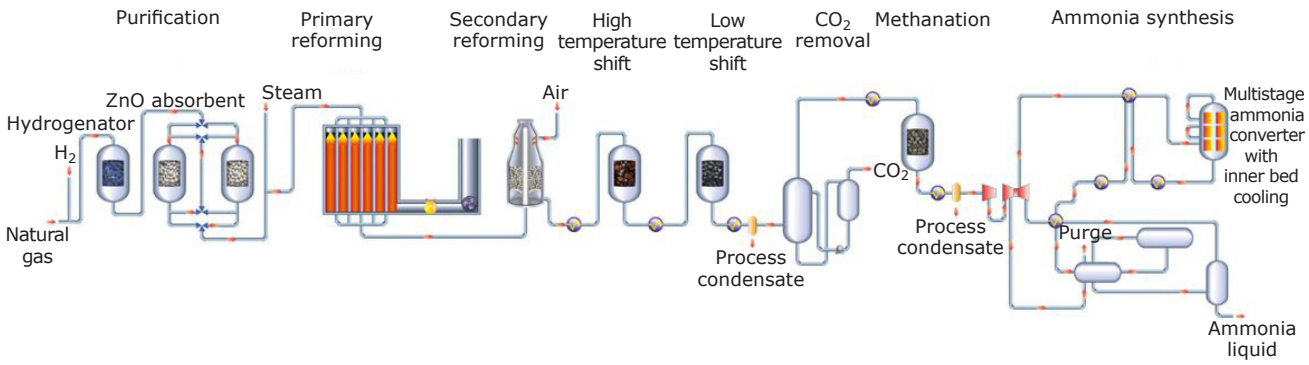


Fig. 1. Conventional syngas route for ammonia production

Equation (i) shows the equilibrium reaction of nitrogen, hydrogen and ammonia:

$$N_2 + 3H_2 \rightleftarrows 2NH_3 \qquad \Delta H_{427^oC} = -52 \text{ kJ mol}^{-1} \quad \text{(i)}$$

The Haber-Bosch process has provided ammonia-based fertiliser to feed our increasing population for a century. Haber-Bosch supports nearly half of global food production and demand for ammonia is expected to increase as the world's population grows (2, 3). The use of ammonia as a carbon-free fuel, or as a hydrogen vector, would also increase demand. Fuel ammonia is a nascent concept but the well-established supply line, stability as a liquid under relatively mild conditions and high hydrogen density make it an attractive zero-carbon fuel (4). Indeed, the use of ammonia as a green fuel could cut carbon emissions from shipping by 50% by 2050 (5–7). As a hydrogen vector, ammonia can be converted to hydrogen (and nitrogen) by catalytic cracking. The resulting hydrogen could be used in fuel cells to generate electricity emitting water as a byproduct (8).

Haber-Bosch and the associated processes require considerable hydrocarbon input and ammonia synthesis is the source of an estimated 1% of global $CO_2$ emissions (9). There is an evident need for the development of ammonia synthesis routes with reduced $CO_2$ emissions if greenhouse gas targets are to be met.

There are several approaches that can be used to decarbonise ammonia. One route would be to capture and store the $CO_2$ emissions associated with conventional synthesis gas (syngas) production, known as blue ammonia. Carbon emissions could be eliminated entirely by supplying green hydrogen to the Haber-Bosch process. Green hydrogen can be produced from the electrolysis of water, which is powered by renewable electricity. There are several recent industrial examples that implement this green hydrogen concept and rapid growth is expected as demand for lower carbon ammonia intensifies (10).

Finally, a more economical route to green ammonia would be to eliminate the Haber-Bosch process entirely and use renewable electrical energy (electrochemical) or sunlight (photochemical) to reduce nitrogen from air to ammonia in the presence of water under ambient conditions. Direct synthesis of green ammonia in this manner is non-trivial owing to the chemical inertness of the nitrogen molecule. It is unlikely to be achievable at the necessary scale and cost to compete with conventional Haber-Bosch or green hydrogen Haber-Bosch for decades. However, green ammonia synthesis could be the most intrinsically economical process because it would not require the combination of electrolysers, air separation units and the high-pressure Haber-Bosch plant (11).

The introduction of these technologies can be understood further by considering them as three

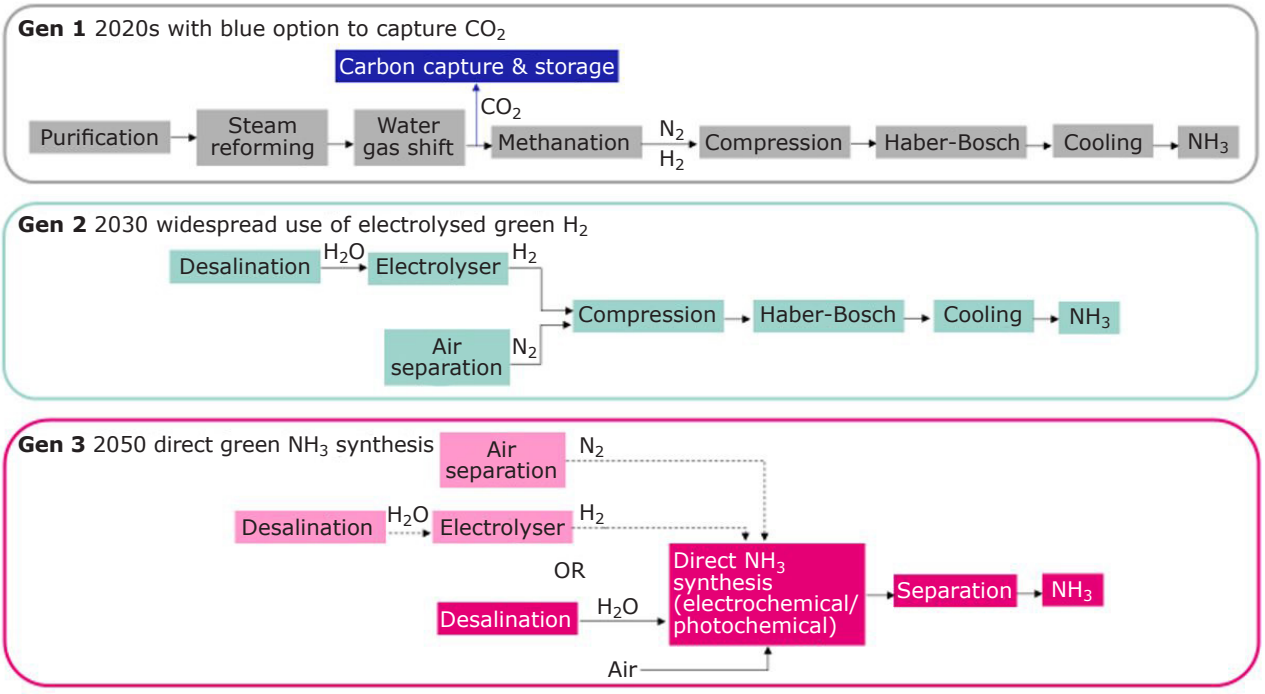


Fig. 2. The generations of ammonia production

generations as presented by Professor Douglas MacFarlane at Monash University, Australia, **Figure 2**. Present day (2020s) ammonia production is Generation 1 with the option of capturing $CO_2$ to make blue ammonia. Generation 2 is electrolysed hydrogen into the conventional process which is predicted to be widespread by 2030. Generation 3 breaks the paradigm of the Haber-Bosch process with direct synthesis of ammonia under mild conditions with a target for commercialisation by 2050 (12).

This review highlights key trends within green ammonia synthesis and identifies opportunities for decarbonisation at the peaks of Generation 2 and Generation 3 (2030 and 2050 respectively). Green hydrogen from the electrolysis of water coupled with an electrically powered Haber-Bosch process (Generation 2) receives considerable attention in the industry already. Several major ammonia producers have announced plans for green ammonia plants though total capacity of the green ammonia projects remains a fraction of the global ammonia production with challenges of high capital investment and access to sufficient renewable energy. With the drive to zero carbon emissions and increasing prominence of ammonia as a hydrogen vector, direct ammonia production (Generation 3) could become widespread.

## 2. Electrolysis of Water to Generate Green Hydrogen for Haber-Bosch

### 2.1 Overview of Green Hydrogen for Ammonia Synthesis

Green ammonia synthesis can be achieved with hydrogen from the electrolysis of water powered by renewable energy. For the process to achieve zero carbon emissions, all aspects of the system must be renewably powered, which includes the compression, heating and separation requirements of the Haber-Bosch process. In addition, desalination of salt water to feed the process must also be considered in areas where access to fresh water is limited.

Equipment and technology vendors offer packages to allow their customers to decarbonise their ammonia plants. For example, contractor and technology provider thyssenkrupp Industrial Solutions (tkIS, Germany) have a strong presence in alkali electrolyser technology and offer a 20 MW electrolyser plant coupled with a 50 tonne $day^{-1}$ ammonia plant (smallest tkIS ammonia plant). Revamp options to existing plants are also offered (13). A further step has been demonstrated by Siemens Energy AG, Germany, with a demonstration unit at the Rutherford Appleton Laboratory in the UK where ammonia is synthesised using Johnson Matthey catalyst in a renewably powered Haber-Bosch process from wind-powered electrolysed hydrogen and nitrogen derived from air separation. The Siemens ammonia is cracked back to hydrogen and fed into fuel cells to derive on-demand electrical power (14).

The current costs of electrolyser technology are high; they have a significant energy demand and upfront cost so improved efficiency in electrolyser technology is a critical development area. **Table I** compares different types of electrolyser to generate green hydrogen for ammonia synthesis. Polymer electrolyte membrane (PEM) electrolysers offer the advantages of high hydrogen purity and pressure to supply the Haber-Bosch process over other technologies as the ammonia synthesis iron catalyst is deactivated by oxygen and ammonia synthesis is favoured at high pressure.

**Table I Comparison of Electrolyser Technologies (15)**

| Electrolysis method | System efficiency, % | Lifetime, kh | Cost, US$ $kW^{-1}$ | Typical pressure, bar | Comments |
|---|---|---|---|---|---|
| **Alkaline (AEL)** | 51–60 | 55–120 | 800–1500 | 10–30 | Mature technology, KOH electrolyte, efficiency decreases at high pressure. Hydrogen purity 99.9% |
| **Proton exchange membrane (PEM) or polymer electrolyte membrane** | 46–60 | 60–100 | 1400–2100 | 20–50 | PEM (Nafion) separates half cells with electrodes mounted on the membrane (membrane electrode assembly). Requires iridium anode and platinum cathode. Hydrogen purity 99.99% |
| **Solid oxide (SO)** | 76–81 | 8–20 | >2000 | 1–15 | Operates 700–900ºC. Highly efficient electrolysis but high temperature material stability is a challenge. |

Three factors are critical for improved cost competitiveness of green hydrogen ammonia: lower electrolyser cost, cheaper renewable energy and carbon taxation. Recent modelling from Professor Bañares-Alcántara at Oxford University, UK suggests green hydrogen ammonia will be cost competitive with conventional Haber-Bosch by 2030 with costs from US$310–1736 tonne$^{-1}$ depending on location and availability of renewable energy. The assessment is made on the basis of the electrolyser cost falling from US$800 kW$^{-1}$ to US$344 kW$^{-1}$, renewable energy costs down by 4.5% for wind and 8.9% for solar, and a carbon tax of US$50 tonne$_{CO2}^{-1}$ (16).

Widespread incorporation of electrolysed hydrogen into green ammonia has prompted consideration of whether the ammonia synthesis process should be operated to match the properties of the green hydrogen feed, for example lower pressure ammonia synthesis. Current electrolysis technology generates hydrogen at maximum 30–50 bar which is compressed for the Haber-Bosch process, in some cases up to 300 bar (17). Electrical compressors supplied with renewable electricity are used in the green ammonia flowsheet so the process remains green. However, the high pressure of the Haber-Bosch loop is beneficial for achieving high conversion of nitrogen and hydrogen to ammonia. High pressure is also favourable for separation, where the ammonia product is removed from the synthesis loop. At high pressure, separation can be achieved with cooling water. At lower pressure, ammonia would condense at much lower temperatures requiring expensive refrigeration systems. For green ammonia, operating condition decisions are likely to be similar to those of conventional syngas-fed Haber-Bosch plants. Syngas plants have similar compression requirements to electrolysed hydrogen and the trade-off between pressure, conversion and separation in the loop must be made. There is variety in syngas ammonia plants with some operating at 300 bar and others a lower pressure, for example 80 bar has been successfully achieved with the Johnson Matthey catalyst KATALCO 74-1. The same variation can be expected for green ammonia with reliance on the Haber-Bosch process expected to dominate.

## 2.2 Alternative Catalysts for the Haber-Bosch Process

Although low pressure ammonia synthesis is unlikely to be suitable for the configuration of conventional Haber-Bosch plants, there may be an opportunity for low pressure systems as demand for non-conventional uses of ammonia rises and if distributed ammonia synthesis develops. There are many examples in academia of research into new catalysts for the Haber-Bosch process. **Table II** provides some recent examples of research into catalysts for the reaction of nitrogen and hydrogen to make ammonia.

**Table II Selected Examples of Ammonia Synthesis Catalyst Development**

| Researchers | Institution | Recent work | Reference |
|---|---|---|---|
| **Professor Hideo Hosono, Professor Michikazu Hara** | Tokyo Institute of Technology, Japan | Ruthenium nanoparticles (12 wt%) on CaFH. Strong interaction of ruthenium and $H^-$ enhanced by inclusion of fluoride promotes nitrogen reduction and results in ammonia synthesis at 50ºC and atmospheric pressure | (18) |
| **Professor Bingyu Lin, Professor Jianxin Lin, Professor Lilong Jiang** | Fuzhou University, China | Enhanced ammonia synthesis of Ru-Ba/a-$Al_2O_3$ compared to performance over g-$Al_2O_3$ equivalent | (19) |
| **Professor Edman Tsang and Ian Wilkinson** | Oxford University, UK and Siemens Plc | Lithium-promoted ruthenium nanoparticles activate nitrogen to ammonia. Nitrogen stabilised by $Li^+$ on ruthenium terrace sites at atmospheric pressure at 460ºC | (20) |
| **Professor Franck Natali** | Victoria University of Wellington, New Zealand | Lanthanide (terbium, gadolinium, praseodymium, dysprosium) metals react with nitrogen to form nitrides which form ammonia when exposed to hydrogen | (21) |
| **Professor Justin Hargreaves** | Glasgow University, UK | $Fe_3Mo_3C$ is an active catalyst for ammonia synthesis above 500ºC owing to lattice carbon substitution by nitrogen | (22) |

## 2.3 Separation of Ammonia from a Low-Pressure Haber-Bosch Process

Separation of ammonia from unreacted nitrogen and hydrogen is a challenge to overcome if low pressure ammonia synthesis is to become viable for two key reasons; the lower yield of ammonia at low pressure and the need to remove it from the system to favour continued reaction of the nitrogen and hydrogen. A summary of potential separation techniques is provided below.

- Absorption - an absorber system could be operated in a 'lead-lag' configuration with one absorption bed picking up ammonia with the other simultaneously regenerated. The use of metal salts as absorbents is an active area of research. For example, $MgCl_2$ will form $MgCl_2$.$NH_3$ at 300ºC and 0.1 bar (23). Metal salts provide a highly selective system for ammonia absorption with high capacity and are able to operate at relatively high temperatures, but the process is likely to be slower than for adsorption
- Adsorption – exploiting the physical interaction of the ammonia molecule with a high surface area structure. There are many examples of ammonia adsorption in literature; activated alumina (24), ionic networks (25) and metal-organic frameworks (26). There are also examples of ammonia adsorption by metals dispersed on high surface area materials (27).

Proof of concept of low-pressure ammonia synthesis integrated with absorption was recently published by Laura Torrente-Murciano at Cambridge University, UK (28). Here, ruthenium (5 wt%) nanoparticles supported on ceria nanorods, promoted with 10% caesium catalysed the ammonia synthesis reaction under relatively mild conditions of 300ºC and 20 bar. The absorbent was composed of manganese chloride supported on silica. The silica support is reported to provide thermal stability to the absorbent, permitting operation at 300ºC. The catalyst and absorbent were loaded in series in discrete sub-beds within the same vessel with a catalyst bed followed by the absorbent followed by a catalyst bed. Ammonia production of the integrated system was higher than that predicted by equilibrium demonstrating favourable catalyst kinetics and absorbent efficacy over the day long period of the experiment. Once the absorbent was saturated with ammonia, it was regenerated with a flow of nitrogen at 360ºC for 2 h.

## 3. Electrochemical Synthesis of Ammonia

Electrochemical ammonia synthesis harnesses electrical energy, which could be renewably sourced, to directly convert the hydrogen of water and nitrogen in air to ammonia at ambient temperature and pressure. If electrochemical ammonia synthesis could be achieved at high efficiency at potentials close to that of the reaction (i.e. low overpotential), it could compete with conventional Haber-Bosch synthesis in terms of overall cost. However, the current level of development for electrocatalytic ammonia synthesis systems is not far advanced beyond laboratory scale.

The recurring challenge for ammonia synthesis is the inertness of the nitrogen molecule. Electrocatalytic reduction of nitrogen requires significant energy input and a catalyst site with strong binding for nitrogen but a weak interaction with ammonia so it is readily released. An additional challenge for electrochemical synthesis is the competing reaction for hydrogen evolution from water rather than hydrogen incorporation into ammonia. An ideal electrocatalyst maximises conversion to ammonia (measured from current density or turnover frequency), has long life, minimises overpotential (electrochemical potential above the thermodynamic potential that is required to drive the reaction) and has a high Faradaic efficiency (FE) (efficiency with which the electric charge is transferred to the electrochemical reaction) (11). The US Department of Energy (US DOE) has set a target rate for viable electrochemical ammonia production of $10^{-4}$ mol $h^{-1}$ $cm^{-1}$ and FE of 50% but current systems suffer from insufficient production rates less than $10^{-6}$ mol $h^{-1}$ $cm^{-1}$ and FE less than 30% indicating how much technology advancement is required. The US DOE estimates that it will take until 2050 for electrochemical ammonia production to compete with Haber-Bosch (30).

If or when electrochemical systems reach the targets, the cost per unit of electrochemical ammonia would be cheaper than that of ammonia from electrolysed hydrogen followed by electrically powered Haber-Bosch. Estimates from Professor Gal Hochman and Professor Alan Goldman from Rutgers University, USA are that if renewable electricity cost is US$50 $MWh^{-1}$, the cost for electrochemical ammonia is ~US$500 $tonne^{-1}$ compared to ~US$630 $tonne^{-1}$ for ammonia

from electrolysed green hydrogen feeding into 2000 tonne day$^{-1}$ Haber-Bosch. The estimate for ammonia from conventional 2000 tonne day$^{-1}$ Haber-Bosch is US$159 tonne$^{-1}$ based on cost of US$2.62 per one thousand British thermal units (MBtu) natural gas (11).

Technoeconomic analysis from Jamie R. Gomez, University of New Mexico, USA, confirms the conclusion that direct electrochemical synthesis of ammonia is intrinsically lower cost than the Haber-Bosch process fed with green hydrogen though the calculated costs differ from those of Hochman and Goldman. Gomez assumes that direct electrochemical synthesis of ammonia will require the same infrastructure as a Haber-Bosch plant: renewably powered hydrogen generation, cryogenic nitrogen separation prior to ammonia synthesis coupled with ammonia liquefication and separation post synthesis. Using the US DOE targets for electrochemical ammonia production of $10^{-4}$ mol $^{-1}$ cm$^{-1}$ and efficiency of 50% and electrochemical reactor operating at 200ºC, ambient pressure, the energy requirement is 17 MWh per tonne of ammonia. The cost of a tonne of electrochemically derived ammonia from this study is US$951 whereas the equivalent process with Haber-Bosch ammonia synthesis was calculated to be US$975 (29).

## 3.1 Electrochemical Ammonia Synthesis Mechanism

The typical electrochemical ammonia synthesis reaction is described by Equation (ii), the nitrogen reduction reaction (NRR):

$$2N_2 + 6H_2O \rightarrow 4NH_3 + 3O_2 \quad \text{(ii)}$$

Reduction of nitrogen occurs at the cathode with six protons and six electrons required to form ammonia (cathode reaction, Equation (iii)). Oxidation of water to hydrogen and oxygen occurs at the anode (anode reaction, Equation (iv)) (11).

$$N_2 + 6H^+ + 6e^- \rightarrow 2NH_3 \quad \text{(iii)}$$

$$3H_2O \rightarrow 1.5O_2 + 6e^- + 6H^+ \quad \text{(iv)}$$

The relatively high number of requisite protons and electrons for nitrogen reduction suggests considerable optimisation is required to improve the reaction kinetics to deliver the charge carriers (30). The mechanism for the reduction of the nitrogen molecule by the six protons and electrons incorporates many intermediates with multiple proton-electron transfer steps. It is likely that electrochemical ammonia synthesis follows an associative mechanism with full cleavage of the nitrogen triple bond after proton-electron transfer, **Figure 3**. The Haber-Bosch process over iron catalysts is known to follow a dissociative mechanism where the first step is nitrogen triple bond breakage. The difference in the mechanisms means that electrochemical ammonia synthesis *via* the NRR is intrinsically lower energy than the Haber-Bosch reaction. The reactions that constitute the NRR together with their potentials are summarised in **Table III** (31). The most negative and therefore most energetically demanding step is the formation of $N_2^-$ (–4.16 V *vs*. normal hydrogen electrode (NHE)). The formation of $N_2H$ is also negative (–3.2 V *vs*. NHE). The negative potentials suggest that these steps are likely to be rate limiting in the electrochemical ammonia synthesis process.

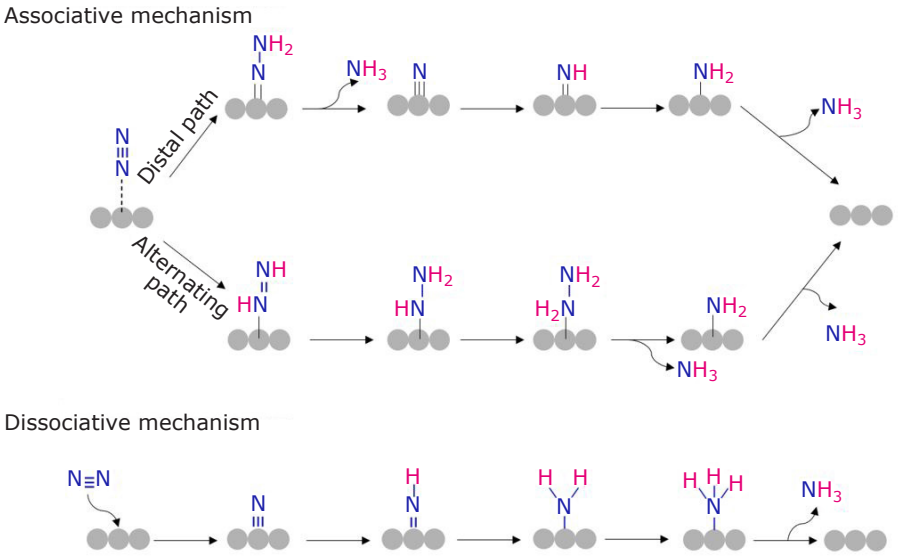


Fig. 3. Possible routes to ammonia *via* the NRR associative mechanism. The dissociative mechanism that occurs over the iron catalyst of the Haber-Bosch process is provided for comparison

**Table III Summary of the Reactions Constituting the Nitrogen Reduction Reaction and Associated Electrode Potentials**

| Reaction | $E^0$, V[a] |
|---|---|
| $H_2O \rightarrow 0.5O_2 + 2H^+ + 2e^-$ | 0.81 *vs.* NHE at pH 7 |
| $2H^+ + 2e^- \rightarrow H_2$ | –0.42 *vs.* NHE at pH 7 |
| $N_2 + e^- \rightarrow N_2^-$ | –4.16 *vs.* NHE at pH 0 |
| $N_2 + H^+ + e^- \rightarrow N_2H$ | –3.2 *vs.* NHE at pH 0 |
| $N_2 + 2H^+ + 2e^- \rightarrow N_2H_2$ | –1.10 *vs.* RHE |
| $N_2 + 4H^+ + 4e^- \rightarrow N_2H_4$ | –0.36 *vs.* NHE at pH 0 |
| $N_2 + 5H^+ + 4e^- \rightarrow N_2H_4^+$ | –0.23 *vs.* NHE at pH 0 |
| $N_2 + 6H^+ + 6e^- \rightarrow 2NH_3$ | 0.55 *vs.* NHE at pH 0 |
| $N_2 + 8H^+ + 8e^- \rightarrow 2NH_4^+$ | 0.27 *vs.* NHE at pH 0 |

[a] NHE is the normal hydrogen electrode, which is the potential of a platinum electrode in 1 M acid solution with hydrogen supplied at 1 atm and at 20ºC. RHE is the reversible hydrogen electrode which is used directly in the electrolyte solution being studied rather than being held at normal conditions and connected to the solution of study by a salt bridge

Theoretical studies are often used to explore the potential mechanisms for electrochemical reactions. Schematic representation of the associative and dissociative mechanisms is presented in **Figure 3**.

The electrochemical system has a significant impact on the efficiency of the process. Factors such as electrode potential, solvent and pH values of electrolytes need to be optimised to achieve the best yields. Electrochemical cell potential is fundamentally dependent on temperature (see box). For the NRR to ammonia from water and nitrogen, the higher the temperature, the lower the potential required to drive the system forward. Electrochemical potential is also critical; different reaction systems tend to have different potentials that will suit ammonia synthesis (33). Furthermore, application of appropriate potential for the NRR can reduce propensity for the hydrogen evolution reaction.

The electrolyte also plays a role. For example, a low pH solution and the ready availability of protons may favour hydrogen evolution over NRR so higher pH might suit some electrochemical ammonia synthesis processes. However, there is no definitive conclusion on the optimal NRR pH range that universally applies to every system.

Catalyst design is also pivotal for achieving the required rates and yields from electrochemical ammonia synthesis. As mentioned, electrocatalysts should have appropriate active sites to bind nitrogen, easily release ammonia and limit the hydrogen evolution reaction. There is intense academic research into catalysts for electrochemical synthesis of ammonia with many reviews summarising progress. The recent paper from Hui Xu of Giner Inc, USA, and Professor Gang Wu of the University at Buffalo, USA (30) and the review by Professor Liang-Xin Ding and Professor Haihui Wang of the South China University of Technology in Guangzhou, China (33) were highly informative. Review papers from Muhammad Aziz from The University of Tokyo, Japan (34) and Sarb Giddey of CSIRO Energy Technology, Australia (35) provide valuable summaries of electrochemical ammonia production. In many cases, advances in nanomaterials have supported recent developments in electrocatalysis. **Table IV** highlights a few recent examples with commentary in the sections below.

## 3.2 Precious Metal Electrocatalysts

Precious metal catalysts (gold, platinum, palladium, rhodium, ruthenium) have promising nitrogen binding energies and excellent conductivity to convey electrons for the reduction reaction.

## Electrochemical Cell Potential

The Nernst equation (Equation (v)) summarises the relationship between reduction potential of an electrochemical reaction to the standard electrode potential, temperature and activities of the chemical species involved.

$$E = E^e - (RT/vF)\ln Q \qquad (v)$$

where F = Faraday's constant ($eN_A$, e = charge of an electron; $N_A$ = Avogadro constant); v = stoichiometric coefficient of electrons in the electrochemical reaction; Q = reaction quotient, product activity/reactant activity; R = molar gas constant; T = temperature in Kelvin (32).

https://doi.org/10.1595/205651322X16334238659301

**Table IV Examples of Electrocatalytic Systems for Generating Ammonia**

| Catalyst | Electrolyte | Faraday efficiency, % | Ammonia production rate, μg $h^{-1}$ $mg_{cat}^{-1}$ | E° *vs.* RHE at 25°C | Comment | Reference |
|---|---|---|---|---|---|---|
| **Pd/C** | 0.1 M phosphate buffered saline (PBS) | 8.24 | 4.5 | –0.2 | Neutral electrolyte (pH 7) improved FE compared to FE of less than 0.1% in NaOH pH 12.9 and $H_2SO_4$ pH 1.2 | (36) |
| **Au-$CeO_2$/ reduced graphene oxide** | 0.1 M HCl | 10.1 | 8.3 | –0.2 | Amorphous gold nanoparticles and structural distortion from ceria provides active sites for NRR | (37) |
| **$Au_1C_3N_4$** | 0.005 $H_2SO_4$ | 11.5 | 1305 | –0.1 | Gold single atom carbon nitride catalyst achieved 22 times more ammonia than equivalent system prepared with gold nanoparticles | (38) |
| **Ru@$ZrO_2$/NC** | 0.1 M HCl | 21 | 183 | –0.2 | Ruthenium single-atom supported on nitrogen-doped porous carbon. $ZrO_2$ supresses hydrogen evolution. Oxygen vacancy sites on $ZrO_2$ promote catalytic activity of ruthenium for ammonia synthesis | (39) |
| **1T-phase $MoS_2$ nanodots on g-$C_3N_4$** | | 20.5 | 30 | –0.3 | 1T $MoS_2$ nano dots possesses high surface area with many active edge sites. Graphitic carbon nitride (g-$C_3N_4$) electronic effect makes catalyst highly selective for NRR | (40) |
| **$Mo_2C$** | 0.1 M HCl | 10 | 95 | –0.2 | Durable catalyst, 58 h operation. Greater FE than other molybdenum catalysts: $MoS_2$ 1.17%, $MoO_3$ 1.9% MoN 1.15% and $Mo_2N$ 4.5%. 25 mA $cm^{-2}$ current efficiency | (41) |
| **FeTPPCl** | 0.1 M $Na_2SO_4$ PBS (phosphate buffered saline) | 17 | 18 | –0.3 | Tetraphenylporphyrin iron chloride. $FeN_4$ site displays strong interaction with nitrogen. Activity retained for 36 h of catalytic testing | (42) |
| **p-$Fe_2O_3$/CC** | 0.1 M $Na_2SO_4$ | 8 | 14 | –0.4 | Porous $Fe_2O_3$ nanorods grown on carbon cloth. Porosity provides facile access to active sites | (43) |
| **$Li^+$/Li** | $Li^+$ in THF | 37 | 28 ppm | –1 *vs.* $Li^+$/Li | $Li^+$ deposited on metal electrode as lithium which reacts with nitrogen in presence of $H^+$ to form ammonia. –3 V required to deposit lithium which makes process unstable. Cycling between potentials for $Li^+$ in solution and deposited lithium has a stabilising effect, 125 h of testing | (44) |
| **LiCl–KCl** | LiCl–KCl–LiH | 4.2 | $2.8 \times 10^{-8}$ mol $cm^{-2}$ $s^{-1}$ | 1 V *vs.* $Li^+$/Li | High rate for electrochemical ammonia synthesis. Molten salt electrolyte with LiH to provide $H^-$. Isotope study to prove $^{15}N_2$ incorporated into $^{15}NH_3$ | (45) |

However, hydrogen evolution often out-completes the NRR over precious metal catalysts (46). Platinum catalysts in particular display a strong propensity for hydrogen evolution rather than nitrogen reduction (36). Hydrogenation of the precious metal surface may be a key first step in the reaction mechanism for NRR over gold and palladium to promote the formation of ammonia from nitrogen (47).

## 3.3 Transition Metal Electrocatalysts

In nature, nitrogenases of nitrogen fixing bacteria catalyse the formation of ammonia from nitrogen with iron and molybdenum identified as the active metals. Iron-only nitrogenase has also been isolated as has a version with molybdenum replaced by vanadium (48). Investigation of electrocatalysts based on iron and molybdenum is a highly active field with promising ammonia rates and FEs. Transition metals have the obvious benefit of lower cost than the precious metal systems.

## 3.4 Molten Salt Electrolytes

Slow kinetics and hydrogen evolution are problems with many of the aqueous systems designed for ammonia synthesis from air and water at ambient temperature and pressure. Systems operated at higher temperature (+100ºC) may have more promise for electrochemical ammonia synthesis at viable rates (49). Molten salt electrolytes have displayed relatively good ammonia synthesis rates with excellent FEs. Of particular interest is a eutectic mixture (a mixture that has a fusion temperature lower than the fusion temperature of any of its components) of LiCl and KCl able to stabilise the $N^{3-}$ ion which would subsequently form ammonia in the presence of a proton source ($H_2$, $H_2O$, HCl) at 400ºC (50). Despite promising prospects for this approach, detailed mechanistic studies put the results into doubt; the reaction to form $N^{3-}$ in the molten salt mixture occurs spontaneously with the species reacting stoichiometrically rather than catalytically. An alternative process with LiCl, KCl and LiH was demonstrated to operate catalytically with LiH providing a hydride $H^-$ to complete the catalytic cycle and undergo oxidation at the anode, see the final entry in **Table IV** (45).

## 3.5 Electrochemical Lithium Metal Cycling

$Li/Li^+$ cycling is another approach that takes advantage of the spontaneous reaction of lithium with nitrogen to form $N^{3-}$ which reacts with a proton source to yield ammonia. Together with lithium's reactivity, its small size is well suited for the diffusion required in electrochemical processes as exploited in the lithium-ion battery industry. Here, a current is applied to reduce $Li^+$ to metallic lithium on an electrode. Metallic lithium reacts with nitrogen to form $N^{3-}$, which is protonated to form ammonia. Various configurations of the system have been reported.

In one set up, the steps are separate to avoid selectivity problems and the hydrogen evolution reaction. Initially, lithium is formed from LiCl-KCl/LiOH-LiCl molten salt hydrolysis at 450ºC in the absence of nitrogen or $H^+$ followed by reaction of lithium with nitrogen to make $Li_3N$ at 100ºC. Finally, $Li_3N$ reacts with $H_2O$ to yield ammonia. LiOH was recovered from the system to demonstrate circularity. The dominant cost in this process is reduction of $Li^+$ to lithium which was achieved at −3 V *vs*. the standard hydrogen electrode (SHE) which is equivalent to 14 kWh $kg^{-1}$ ammonia which at US$50 $MWh^{-1}$ electricity cost, corresponds to US$700 $tonne^{-1}$ ammonia (44).

Lithium metal cycling has its challenges, constant deposition of lithium leads to the formation of a lithium-containing passivation layer or solid electrolyte interface (SEI) layer through a reaction of lithium with the organic solvent electrolyte which impedes current flow. To overcome this barrier, experiments have shown that switching electrochemical potential between a lithium deposition regime and $Li^+$ in solution leads to a more stable process. The electrochemical potential cycling technique also favours ammonia production because electron availability to reduce nitrogen is enhanced during the $Li^+$ solution phase. The system was demonstrated to generate ammonia over 125 h with the highest reported FE of 37% using deposition current −2 mA $cm^{-2}$ applied for 1 min followed by up to 8 min of resting potential at 0 V *vs*. $Li/Li^+$. The SEI formed here is also beneficial as it helps control diffusion of $Li^+$, protic species, nitrogen and ammonia. Once formed, it also prevents excessive degradation of the electrolyte (ethanol in this particular study) by providing a barrier between the organic species and lithium metal.

## 3.6 Electrocatalysis Summary

Significant development is required before electrochemical ammonia synthesis will replace the Haber-Bosch process. The substantial

 

thermodynamic challenge to activate nitrogen requires highly active catalysts that do not simultaneously catalyse the reduction of water to hydrogen. It is likely that a combination of careful catalyst design and electrochemical system control will be needed for the process to succeed. Economic assessments indicate that an active and efficient electrochemical ammonia synthesis process would compete financially with electrolysed hydrogen feeding Haber-Bosch with 2050 the estimate for viable technology readiness. A variety of catalysts and electrochemical systems have been discussed in this section with gold nanomaterials and lithium metal cycling promising candidates though further breakthroughs are required to achieve the performance needed for a production plant. Effective separation techniques to isolate ammonia from the electrolyte solution would also be required.

## 4. Photochemical Ammonia Synthesis

Photochemical reactions are driven by light and photocatalysed ammonia synthesis is regarded as a potential route to green ammonia. The benefit of photocatalysis is that energy for the reaction would be provided directly from sunlight with water and air to provide hydrogen and nitrogen respectively. Unlike the electrochemical process, there would be no need to supply electricity, making photochemical synthesis a potential candidate for decentralised off-grid ammonia production. An evident drawback of photochemical processes is that they only operate when the sun is shining.

The concept would likely feature the catalyst dispersed in a panel to optimise light exposure, potentially suspended in water or as a coated catalyst with water and air bubbled over the surface. Ammonia would need to be separated from the mixture before application as a fertiliser. Photocatalytic activities of ~500 $mmol_{NH3}$ $g_{cat}^{-1}$ $h^{-1}$ (51) have been reported from the current state of the art systems which is 1000 times less than the electrochemical systems. As **Table V** indicates, the area of a coated 500 $mmol_{NH3}$ $g_{cat}^{-1}$ $h^{-1}$ photocatalyst required to match a 2000 tonne per day Haber-Bosch plant would be 1265 $km^2$, a considerable area equivalent to the North York Moors National Park in the UK. A 100-fold improvement in catalyst activity would reduce the area required to 13 $km^2$ which would be a more feasible area to cover. For comparison, the world's largest solar park at the time of writing is 57 $km^2$ at Bhadla, India (52).

As mentioned, photocatalysis might suit demands of off-grid distributed ammonia production. In this case ammonia demand would be significantly less than a 2000-tonne-per day plant. Agricultural fertiliser demands vary according to crop, soil type and geography but if nitrogen requirement of 200 kg nitrogen $hectare^{-1}$ $year^{-1}$ (53) is used as a conservative average and 400 hectares the size of a large arable farm (54), the quantity of ammonia required is ~100 tonnes $year^{-1}$. With a 500 $mmol_{NH3}$ $g_{cat}^{-1}$ $h^{-1}$ coated photocatalyst, the area required is 0.2 $km^2$ or 20 hectares, 5% of the size of the farm.

A complicating factor is that molecular ammonia is rarely applied as a fertiliser. Its high volatility and solubility mean it would rapidly evaporate or leach away. Ammonia is converted to a range of compounds such as urea or ammonium salts (for example, $(NH_4)_2SO_4$ or $NH_4NO_3$) to be applied as a fertiliser. Distributed ammonia production would need additional technology for conversion

**Table V Estimated Area Required for a Photocatalyst to Produce 2000 tonnes $day^{-1}$ Ammonia**

| | Unit | Current best catalyst activity | Activity increase by 10 | Activity increase by 100 |
|---|---|---|---|---|
| **Photocatalyst layer** | microns | 10 | 10 | 10 |
| **Typical coated catalyst loading** | mg $m^{-2}$ | 15500 | 15500 | 15500 |
| | g $m^{-2}$ | 15.5 | 15.5 | 15.5 |
| **Catalyst activity** | mmol $g^{-1}$ $h^{-1}$ | 500 | 5000 | 50,000 |
| **Ammonia from 1 $m^2$ in 1 h** | mmol | 7750 | 77500 | 775000 |
| | mg | 131750 | 1317500 | 13175000 |
| | g | 0.13175 | 1.3175 | 13.175 |
| **Ammonia in 12 h daylight** | g | 1.581 | 15.81 | 158.1 |
| | tonnes | 1.581E-06 | 1.58E-05 | 0.000158 |
| **Area required for 2000 tonnes $day^{-1}$ ammonia plant** | $m^2$ | 1.265E+09 | 1.27E+08 | 12650221 |
| | $km^2$ | 1265 | 127 | 13 |

of ammonia to fertiliser compounds. Furthermore, different fertiliser compounds have varying $CO_2$ emissions associated with their production and use. The $CO_2$ emissions from urea are 8% higher than from ammonium nitrate (55). However, ammonium nitrate can be highly explosive if not manufactured, stored and handled properly according to recognised standards and decentralised production poses significant safety and security risks. Together with advances in ammonia production, decentralisation also requires developments in fertiliser compounds, their application and stability and ease of production from ammonia.

## 4.1 Mechanism of Photocatalytic Ammonia Synthesis

Highly active photocatalysts are required to enable photochemical ammonia synthesis to become a viable process. Photocatalysts often rely on semi-conductor materials to absorb solar energy. The energy excites photo-induced electrons into the semi-conductor conduction band and leaves holes in the valence band. The electrons in the conduction band are available for reducing nitrogen to ammonia through migration to the catalyst active site where nitrogen is bound. The holes provide charge balance and complete the catalytic cycle with the oxidation of $H_2O$ to $O_2$ (56). The process is summarised in **Figure 4**. A complication with photocatalytic ammonia synthesis is that the rate of hole quenching with water to complete the catalytic cycle is slow so hole scavengers such as methanol or formaldehyde can be used instead to achieve a faster rate for the photochemical reaction.

As with electrocatalysed ammonia synthesis, it is likely that the reaction follows an associative mechanism with hydrogenation of adsorbed nitrogen prior to cleavage of the nitrogen-nitrogen bond. Exact mechanisms are likely to differ depending on the configuration of the various catalytic processes. Hydrogen evolution remains a strong competing reaction. A significant thermodynamic barrier to overcome is the reduction potential of $N_2 + e^- \rightarrow N_2^-$ –4.2 eV (**Table III**). The conduction band gap of many semiconductors should be greater than this energy requirement so semiconductor choice is key for photocatalysis design (57).

Quantum efficiency (QE) is another critical factor for photochemical processes and describes the proportion of photons incident on a semiconductor that go on to excite electrons and reduce nitrogen in the case of photochemical ammonia synthesis. Owing to the challenge of variation in equipment and catalytic setups, incident light intensity rather than absorbed light intensity is used to calculate apparent QE (58).

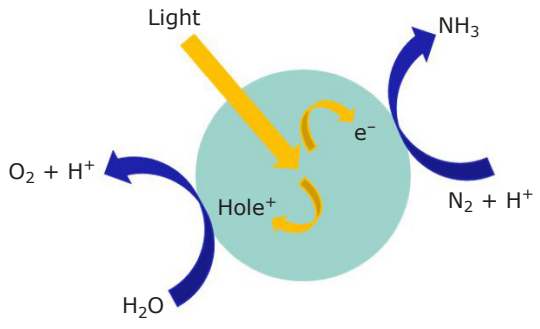


Fig. 4. Photocatalytic generation of ammonia and oxygen following light activation of a semiconductor and generation of electrons and holes

## 4.2 Photochemical Ammonia Synthesis Catalysts

A comparison of a variety of photocatalysts for ammonia generation is provided in **Table VI** with a more detailed discussion of the photocatalysts in the next section. Several thorough reviews of photochemical ammonia synthesis catalysts have recently been published including one from Professor Junwang Tang from University College London, UK (53), one from Professor Tierui Zhang from the Chinese Academy of Sciences, Beijing, China (62) and another from Professor Zhong Jin from Nanjing University, China (54).

### 4.2.1 Defect Incorporation

Vacancies in a photocatalyst can improve nitrogen adsorption and charge separation of photoexcited electrons and associated holes. For example, oxygen vacancies in BiOBr nanosheets promote the electron transfer to adsorbed nitrogen and enhance ammonia generation compared to the BiOBr material without vacancies. The BiOBr nanosheet is composed of $[Bi_2O_2]^{2-}$ units interleaved with bromine atoms with a band gap of 2.8 eV which corresponds to visible light absorption. The oxygen vacancies were formed through the reaction of ethylene glycol with surface oxygen in BiOBr. An ammonia production rate of 104 μmol $h^{-1}$ $g_{cat}^{-1}$ was measured (63).

**Table VI Examples of Photocatalytic Systems for the Generation of Ammonia**

| Catalyst | Quantum efficiency, % | Ammonia production rate, μmol $h^{-1}$ $g_{cat}^{-1}$ | Scavenger | Comment | Reference |
|---|---|---|---|---|---|
| **BiOBr nanosheet with oxygen vacancies** | 0.23 at 420 nm | 104 | None | Oxygen vacancies of BiOBr nanosheets activate adsorbed nitrogen. Enhanced electron density at oxygen vacancy suppresses electron/hole recombination and promotes electron transfer to nitrogen for reduction to ammonia. Experiment preceded by theoretical study to confirm feasibility. Oxygen generation was detected proving $H_2O$ able to act as electron donor | (59) |
| **FePt@$C_3N_4$** | 0.15 at 450–500 nm | 4 | None | Platinum doping of $FeC_3N_4$ nanoclusters enhances nanocluster morphology by preventing agglomeration of magnetic particles and improves electron/hole charge separation to enhance nitrogen reduction | (60) |
| **SV-1T-$MoS_2$-CdS nanorod** | 4.4 at 420–780 nm | 457 | Methanol | Oxygen doped 1T-$MoS_2$ nanosheets with sulfur vacancies (SV) deployed as cocatalysts over CdS nanorods. SVs and metallic conduction properties of 1T-$MoS_2$ promotes electron/hole separation. The SV-1T-$MoS_2$ also provides active sites for nitrogen binding | (61) |
| **CdS-Fe-s$MoS_2$** | 3.5 at 436 nm | 459 | None | CdS 10 nm quantum dots as cocatalyst for single-atom iron on single layer $MoS_2$. Electron/holes generated by CdS and efficiently separated at Fe-$S_2$-Mo interface | (51) |

### 4.2.2 Metal Doping

A photocatalyst composed of iron-platinum loaded graphitic carbon nitride (g-$C_3N_4$) displays ammonia production rate of 4 μmol $h^{-1}$ $g_{cat}^{-1}$. Graphitic carbon nitride is derived from urea and has semiconductor properties. The prepared catalyst contained 0.3 wt% platinum and 3 wt% iron on g-$C_3N_4$ and is designated FePt@$C_3N_4$. The addition of platinum prevented agglomeration of the nanoclusters compared to the equivalent Fe@$C_3N_4$ species. Platinum doping also causes an uplift in the semiconductor energy band which improves electron/hole separation favouring electron conduction to bound nitrogen and its subsequent reduction. Photocatalytic activity was tested in the presence of hydrogen and nitrogen with formation of $N_2H_4$ considered indicative of potential to make ammonia (60).

### 4.2.3 Cocatalyst Incorporation

Cocatalysts are used in photocatalytic processes to enhance the photostability of catalysts. For example, cadmium sulfide has received considerable attention as a photocatalyst. It has favourable band positions and is relatively simple to prepare but it is readily oxidised and corrodes when exposed to light. Photocatalytic efficiency of cadmium sulfide is also low owing to rapid electron/hole recombination. Combining cadmium sulfide with a cocatalyst can enhance its properties. In one example cadmium sulfide nanorods prepared by precipitation were combined with 30% oxygen-doped 1T-MoS nanosheets with sulfur vacancies (SV-1T-$MoS_2$) also prepared by a hydrothermal reaction and precipitation (61).

Another cocatalyst example is provided by CdS-Fe-s$MoS_2$ from the research group of Professor Edman Tsang at Oxford University, UK and patented by Oxford University Innovation. The photocatalyst displays relatively good activity of 459 μmol $h^{-1}$ $g_{cat}^{-1}$ and high quantum yield of 3.5%. It is composed of cadmium sulfide quantum dots incorporated onto single-atom iron on single layer molybdenum sulfide. The combination of the component units raises the system's valence

 

band to a potential that exceeds nitrogen reduction (–4.2 *vs*. NHE at pH 0) so electrons are of appropriate energy to reduce nitrogen. The single layer molybdenum sulfide catalyst is made from bulk molybdenum sulfide by lithium intercalation and sonication in water. Single atom iron doping of the s-$MoS_2$ is achieved hydrothermally before combining with 10 nm particles of cadmium sulfide. The cadmium sulfide particles provide additional catalytic activity, likely though the contribution of additional electron-hole pairs from visible light illumination. Efficient separation of the electron and holes is achieved by the [Fe-$S_2$-Mo] motifs in Fe-s$MoS_2$ at the materials' interface.

## 4.3 Photocatalysis Summary

A photocatalytic route to ammonia is likely to be even further off than electrocatalytic ammonia synthesis. Photocatalytic activity is roughly 1000 times less than the electrocatalysts. Breakthroughs in catalyst development are required to achieve adequate ammonia synthesis rates. More active photocatalysts would enable installations of reasonable and practical size to capture the required solar energy to make economically competitive quantities of ammonia. The opportunity for photochemical ammonia synthesis in isolated locations to make fertiliser is questionable considering ammonia's toxicity and high solubility, requiring its conversion to fertiliser compounds before application on farmers' fields. Truly decentralised ammonia production would need to be coupled with fertiliser compound synthesis which may delay realisation of the concept.

Despite the challenges, a photocatalytic system would be 'super green', powered by sunlight and synthesising ammonia from air and water without direct power requirements. In locations benefitting from high sunlight levels, photocatalytic ammonia synthesis could provide a production boost to an existing ammonia facility. As for electrocatalysis, successful photocatalytic systems are based on nano-systems with strong propensity to bind and activate nitrogen and optimised to conduct photo-induced electrons to the catalyst active site. A system based on CdS-Fe-s$MoS_2$ was recently patented by Oxford Innovations UK and has among the highest ammonia production rates reported.

# 5. Conclusions

Green routes to ammonia are receiving considerable attention from academia, governments and industry to mitigate the high carbon footprint of the conventional Haber-Bosch process which is estimated to contribute 1% of global $CO_2$ emissions. Many key players of the ammonia industry have already announced plans to incorporate green hydrogen from electrolysis into their existing plants. It is likely that more will follow.

The development of lower pressure ammonia synthesis systems (less than 20 bar) is also an area receiving attention though the current industrial trend is towards higher pressure systems owing to the challenges of separating ammonia at low pressure and lower conversion. However, there may be instances where smaller, lower pressure plants make sense. These plants would require catalyst development to operate at the lower pressure and novel separation techniques to isolate the product ammonia.

Although direct ammonia synthesis *via* electro- or photocatalysis is a distant prospect, the gains to be made are significant considering that the direct route from water and air or (hydrogen and nitrogen) is inherently lower cost than electrolysis and Haber-Bosch. Efforts on direct ammonia synthesis would be a long-term undertaking as the technology is not anticipated to be economically viable for another 30 years. However, if ammonia demand for fertilisers and fuel increases as expected, production at lower cost with zero carbon emissions presents an attractive opportunity. Furthermore, the pursuit of intrinsically lower cost routes to ammonia synthesis such as electrochemical or photochemical will drive innovation in these fields which may accelerate breakthroughs. If ammonia is to be produced from water and air, separation techniques to isolate ammonia will be critical here too.

# References

1. J. R. Jennings and S. A. Ward, 'Ammonia Synthesis: Thermodynamics of Ammonia Synthesis: Process Consequences', in "Catalyst Handbook", 2nd Edn., ed. M. V. Twigg, CRC Press, Boca Raton, USA, 1996, p. 390
2. 'The Future of Food and Agriculture: Trends and Challenges', Issue 1, Food and Agriculture

 

Organization of the United Nations, Rome, Italy, 2017, 163 pp

3. J. W. Erisman, M. A. Sutton, J. Galloway, Z. Klimont and W. Winiwarter, *Nat. Geosci*., 2008, **1**, (10), 636
4. M. Aziz, A. T. Wijayanta and A. B. D. Nandiyanto, *Energies*, 2020, **13**, (12), 3062
5. T. Brown, 'US House Draft Bill Defines Ammonia as Low-Carbon Fuel', Ammonia Energy Association, New York, USA, 13th February, 2020
6. "Ammonia: Zero-Carbon Fertiliser, Fuel and Energy Store: Policy Briefing", The Royal Society, London, UK, 19th February, 2020, 39 pp
7. T. Ayvalı, S. C. E. Tsang and T. Van Vrijaldenhoven, *Johnson Matthey Technol. Rev*., 2021, **65**, (2), 291
8. B. Lee, J. Park, H. Lee, M. Byun, C. W. Yoon and H. Lim, *Renew. Sustain. Energy Rev*., 2019, **113**, 109262
9. P. Gilbert and P. Thornley, 'Energy and Carbon Balance of Ammonia Production from Biomass Gasification', University of Manchester, UK, 2010, 9 pp, in *host publication*
10. W. Thomas, 'Fertiliser Industry Takes Leap of Faith on Green Ammonia', CRU International Limited, London, UK, 25th June, 2021
11. G. Hochman, A. S. Goldman, F. A. Felder, J. M. Mayer, A. J. M. Miller, P. L. Holland, L. A. Goldman, P. Manocha, Z. Song and S. Aleti, *ACS Sustain. Chem. Eng*., 2020, **8**, (24), 8938
12. D. R. MacFarlane, P. V. Cherepanov, J. Choi, B. H. R. Suryanto, R. Y. Hodgetts, J. M. Bakker, F. M. Ferrero Vallana and A. N. Simonov, *Joule*, 2020, **4**, (6), 1186
13. C. Schwiderek, Thyssenkrupp, 'Green Ammonia Technology', $NH_3$ Event, 4th European Power to Ammonia Conference, Rotterdam, The Netherlands, 3rd–4th June, 2021
14. "'Green' Ammonia is the Key to Meeting the Twin Challenges of the 21st Century', Siemens-Energy AG, Munich, Germany: https://www.siemens-energy.com/uk/en/offerings-uk/green-ammonia.html (Accessed on 1st February 2021)
15. A. Buttler and H. Spliethoff, *Renew. Sustain. Energy Rev*., 2018, **82**, (3), 2440
16. R. M. Nayak-Luke and R. Bañares-Alcántara, *Energy Environ. Sci*., 2020, **13**, (9), 2957
17. C. Smith, A. K. Hill and L. Torrente-Murciano, *Energy Environ. Sci*., 2020, **13**, (2), 331
18. M. Hattori, S. Iijima, T. Nakao, H. Hosono and M. Hara, *Nat. Commun.*, 2020, **11**, 2001
19. B. Lin, L. Heng, B. Fang, H. Yin, J. Ni, X. Wang, J. Lin and L. Jiang, *ACS Catal.*, 2019, **9**, (3), 1635
20. J. Zheng, F. Liao, S. Wu, G. Jones, T.-Y. Chen, J. Fellowes, T. Sudmeier, I. J. McPherson, I. Wilkinson and S. C. E. Tsang, *Angew. Chem. Int. Ed.*, 2019, **58**, (48), 17335
21. J. R. Chan, S. G. Lambie, H. J. Trodahl, D. Lefebvre, M. Le Ster, A. Shaib, F. Ullstad, S. A. Brown, B. J. Ruck, A. L. Garden and F. Natali, *Phys. Rev. Mater.*, 2020, **4**, (11), 115003
22. A. Daisley and J. S. J. Hargreaves, *J. Energy Chem.*, 2019, **39**, (12), 170
23. C. Smith, A. V. McCormick and E. L. Cussler, *ACS Sustain. Chem. Eng*., 2019, **7**, (4), 4019
24. D. Saha and S. Deng, *J. Chem. Eng. Data*, 2010, **55**, (12), 5587
25. X. Luo, R. Qiu, X. Chen, B. Pei, J. Lin and C. Wang, *ACS Sustain. Chem. Eng*. 2019, **7**, (11), 9888
26. T. N. Nguyen, I. M. Harreschou, J.-H. Lee, K. C. Stylianou and D. W. Stephan, *Chem Commun*., 2020, **56**, (67), 9600
27. A. M. B. Furtado, Y. Wang, T. G. Glover and M. D. LeVan, *Micro. Meso. Mater*., 2011, **142**, (2–3), 730
28. C. Smith and L. Torrente-Murciano, *Adv. Energy Mater*., 2021, **11**, (13), 2003845
29. J. R. Gomez, J. Baca and F. Garzon, *Int. J. Hydro. Energy*, 2020, **45**, (1), 721
30. H. Xu, K. Ithisuphalap, Y. Li, S. Mukherjee, J. Lattimer, G. Soloveichik, and G. Wu, *Nano Energy*, 2020, **69**, 104469
31. X. Chen, N. Li, Z. Kong, W.-J. Ong and X. Zhao, *Mater. Horiz*., 2018, **5**, (1), 9
32. P. W. Atkins and J. De Paula, "Physical Chemistry", 8th Edn., Oxford University Press, Oxford, UK, 2006, p. 221
33. M. Wang, S. Liu, T. Qian, J. Liu, J. Zhou, H. Ji, J. Xiong, J. Zhong and C. Yan, *Nat. Commun*., 2019, **10**, 341
34. F. B. Juangsa, A. R. Irhamna and M. Aziz, *Int. J. Hydro. Energy*, 2021, **46**, (27), 14455
35. S. Giddey, S. P. S. Badwal and A. Kulkarni, *Int. J. Hydro. Energy*, 2013, **38**, (34), 14576
36. G.-F. Chen, S. Ren, L. Zhang, H. Cheng, Y. Luo, K. Zhu, L.-X. Ding and H. Wang, *Small Meth*., 2019, **3**, (6), 1800337
37. S.-J. Li, D. Bao, M.-M. Shi, B.-R. Wulan, J.-M. Yan and Q. Jiang, *Adv. Mater.*, 2017, **29**, (33), 1700001
38. X. Wang, W. Wang, M. Qiao, G. Wu, W. Chen, T. Yuan, Q. Xu, M. Chen, Y. Zhang, X. Wang, J. Wang, J. Ge, X. Hong and Y. Li, *Sci. Bull.*, 2018, **63**, (19), 1246
39. H. Tao, C. Choi, L.-X. Ding, Z. Jiang, Z. Han, M. Jia, Q. Fan, Y. Gao, H. Wang, A. W. Robertson, S.

 

Hong, Y. Jung, S. Liu and Z. Sun, *Chem*, 2019, **5**, (1), 204

40. X. Xu, X. Tian, B. Sun, Z. Liang, H. Cui, J. Tian and M. Shao, *Appl. Catal. B: Environ.*, 2020, **272**, 118984
41. X. Ren, J. Zhao, Q. Wei, Y. Ma, H. Guo, Q. Liu, Y. Wang, G. Cui, A. M. Asiri, B. Li, B. Tang and X. Sun, *ACS Cent. Sci.*, 2019, **5**, (1), 116
42. X. Yang, S. Sun, L. Meng, K. Li, S. Mukherjee, X. Chen, J. Lv, S. Liang, H.-Y. Zang, L.-K. Yan and G. Wu, *Appl. Catal. B: Environ.*, 2021, **285**, 119794
43. Z. Wang, K. Zheng, S. Liu, Z. Dai, Y. Xu, X. Li, H. Wang and L. Wang, *ACS Sustain. Chem. Eng.*, 2019, **7**, (13), 11754
44. S. Z. Andersen, M. J. Statt, V. J. Bukas, S. G. Shapel, J. B. Pedersen, K. Krempl, M. Saccoccio, D. Chakraborty, J. Kibsgaard, P. C. K. Vesborg, J. Nørskov and I. Chorkendorff, *Energy Environ. Sci.*, 2020, **13**, (11), 4291
45. I. J. McPherson, T. Sudmeier, J. P. Fellowes, I. Wilkinson, T. Hughes and S. C. E. Tsang, *Angew. Chem. Int. Ed*., 2019, **58**, (48), 17433
46. J. Wang, S. Chen, Z. Li, G. Li and X, Liu, *ChemElectroChem*, 2020, **7**, (5), 1067
47. C. Y. Ling, Y. Zhang, Q. Li, X. Bai, L. Shi and J. Wang, *J. Am. Chem. Soc*., 2019, **141**, (45), 18264
48. B. M. Hoffman, D. Lukoyanov, Z.-Y. Yang, D. R. Dean and L. C, Seefeldt, *Chem. Rev*., 2014, **114**, (8), 4041
49. V. Kyriakou, I. Garagounis, E. Vasileiou, A. Vourros and Stoukides, *Catal. Today*, 2017, **286**, 2
50. T. Murakami, T. Nishikiori, T. Nohira and Y. Ito, *J. Am. Chem. Soc*., 2003, **125**, (2), 334
51. S. C. E. Tsang and J. Zheng, Oxford University Innovation Ltd, 'Photocatalyst', *World Patent Appl.* 2020/193,951
52. P. Sanjay, 'With 2,245 MW of Commissioned Solar Projects, World's Largest Solar Park is Now at Bhadla', Mercom, India, 19th March, 2020
53. K. Sieling, O. Günther-Borstel and H. Hanus, *J. Agri. Sci*., 1997, **128**, (1), 79
54. M. B. Ali, N. L. Brooks and R. G. McElroy, 'Characteristics of US Wheat Farming: A Snapshot', Statistical Bulletin No. SB 968, United States Department of Agriculture, Washington, DC, USA, June, 2000, 61 pp
55. F. Brentrup, A. Hoxha and B. Christensen, 'Carbon Footprint Analysis of Mineral Fertiliser Production in Europe and Other World Regions', 10th International Conference on Life Cycle Assessment of Food, University College Dublin, Ireland, Dublin, 19th–21st October, 2016, 9 pp
56. Q. Han, H. Jiao, L. Xiong and J. Tang, *Mater. Adv*., 2021, **2**, (2), 564
57. X. Xue, R. Chen, C. Yan, P. Zhao, Y. Hu, W. Zhang, S. Yang and Z. Jin, *Nano Res*., 2019, **12**, (6), 1229
58. H. Kisch and D. Bahnemann, *J. Phys. Chem. Lett*., 2015, **6**, (10), 1907
59. H. Li, J. Shang, Z. Ai and L. Zhang*, J. Am. Chem. Soc.*, 2015, **137**, (19), 6393
60. Z. Li, Z. Gao, B. Li, L. Zhang, R. Fu, Y. Li, X. Mu and L. Li, *Appl. Catal. B: Environ*., 2020, **262**, 118276
61. B. Sun, Z. Liang, Y. Qian, X. Xu, Y. Han and J. Tian, *ACS Appl. Mater. Interfaces*, 2020, **12**, (6), 7257
62. S. Zhang, Y. Zhao, R. Shi, G. I. N. Waterhouse and T. Zhang, *EnergyChem*, 2019, **1**, (2), 100013
63. H. Li, J. Shang, Z. Ai and L. Zhang, *J. Am. Chem. Soc*., 2015, **137**, (19), 6393

## The Author

Katie Smart has a PhD in Chemistry from the University of Paul Sabatier, France, where she studied at the Laboratoire de Chimie de Coordination in Toulouse. Katie has worked at Johnson Matthey since 2013 and is currently Technical Development Manager for the Ammonia Synthesis and High-Temperature Shift R&D teams at the Chilton site in Billingham, UK.

 